Reprinted from J. Chem. Phys. 37 (1962) 2631-2645
by permission of the American Institute of Physics and author(s)

Charge Exchange between Gaseous Ions and Atoms

DONALD RAPP AND W. E. FRANCIS
Lockheed Missiles and Space Company, Palo Alto, California

(Received March 28, 1962)

A calculation of symmetric resonant charge exchange cross sections has been made for a selection of atoms in the velocity range where the impact parameter method is applicable. Cross sections for other atoms can be estimated by interpolating in terms of their ionization potentials. The results are in fair agreement with experiment. A similar calculation has been attempted for asymmetric nonresonant charge exchange processes. The approximations used are more restrictive in this calculation, the calculations being only semiquantitative in nature. The cross section of an asymmetric charge exchange process is determined in terms of the ΔE of the reaction and the "average" ionization potential of the two atoms. The results are qualitatively in agreement with experiment. A very brief discussion of approaches for extrapolating data to lower velocities, where the rectilinear orbit impact parameter method is not applicable, is given.

I. INTRODUCTION

THE charge transfer processes we consider are symmetric resonant,

$$A+A^+\rightarrow A^++A, \tag{1}$$

and asymmetric nonresonant,

$$A+B^+\rightarrow A^++B+\Delta E, \tag{2}$$

where ΔE is the difference in ionization potentials of B and A. Process (1) has been the subject of intensive research, and a large number of theoretical papers dealing with such reactions have been published. No important contributions to the theory of process (1) are made here. Instead, our purpose is to develop an improved *a priori* calculation of cross sections for a wide variety of processes (1) in terms of theory that is already available. Process (2) has been considered in only a relatively few instances, and because of the lack of an available detailed theory, both conceptual and computational developments have been attempted.

The calculations are based on several approximations which are explicitly stated. No adjustable parameters are involved, and the *a priori* computations are judged on the basis of a comparison with available experimental data. In some cases the absolute agreement may be poor. However, it is felt that the general dependence of cross sections for processes (1) and (2) on ion velocity is correctly predicted in this paper. It is hoped that such a semiquantitative characterization of a wide range of charge-transfer processes proves to be of value, both in leading to general understanding of the phenomena and in extrapolating experimental data beyond the range of measurements.

II. RANGES OF ION VELOCITY

It is convenient to delineate three ranges of ion velocity[1] for charge transfer. The most often considered velocity range is "intermediate," for which the ion velocity is high enough that Jeffrey's approximation can be applied to the quantum-mechanical collision dynamics.[2] The result is equivalent to the semiclassical impact-parameter method.[2-4] For "high" ion velocities the electron orbital velocity in the atom is no longer (relatively) large enough to use the Born–Oppenheimer separation of electronic and atomic motions. The consequence of this complication is to reduce the cross section below that predicted by the usual impact-parameter method. A general procedure which gives reasonable results at high velocities, and which reduces to the usual impact-parameter treatment at intermediate velocities, has been proposed[5] and recently applied.[6] The "high" and "intermediate" regions overlap at about $v\approx 10^8$ cm/sec. We confine most of our attention to velocities below this value and do not utilize the methods developed for the "high" velocity region. At "low" velocities, Jeffrey's approximation (for high phase shifts) cannot be applied since only the low phase shifts are of importance. Only a rigorous wave-mechanical treatment is valid. However, if a semiclassical method is to be used in this region for approximate calculations, it should take into account the curved classical orbits instead of assuming rectilinear orbits as in the usual impact-parameter method.[1] Since the long-range force between an ion and atom is attractive, such a method tends to make the cross section higher than that predicted by the usual impact-parameter method. The "dividing line" between "low" and "intermediate" velocity regions varies from case to case. An approximate analysis given in Sec. VI leads to roughly $(10^5/\mu^{\frac{1}{2}})$ cm/sec, with μ the reduced mass (in amu) of the collision pair. In this paper we mainly consider velocities in excess of this value. The "low"

[1] This proposal was made by J. L. Magee and D. Rapp, Proc. 2nd Intern. Symp. on Electronic and Atomic Impact Phenomena, Boulder, Colorado, June 1961.

[2] D. R. Bates, H. S. W. Massey, and A. L. Stewart, Proc. Roy. Soc. (London) **A216**, 437 (1953).

[3] E. F. Gurnee and J. L. Magee, J. Chem. Phys. **26**, 1237 (1957).

[4] K. Takayanagi, Repts. Progr. Saitama Univ. **AII**, 33 (1955).

[5] D. R. Bates and R. McCarrol, Proc. Roy. Soc. (London) **A245**, 175 (1958).

[6] R. McCarrol, reference 1.

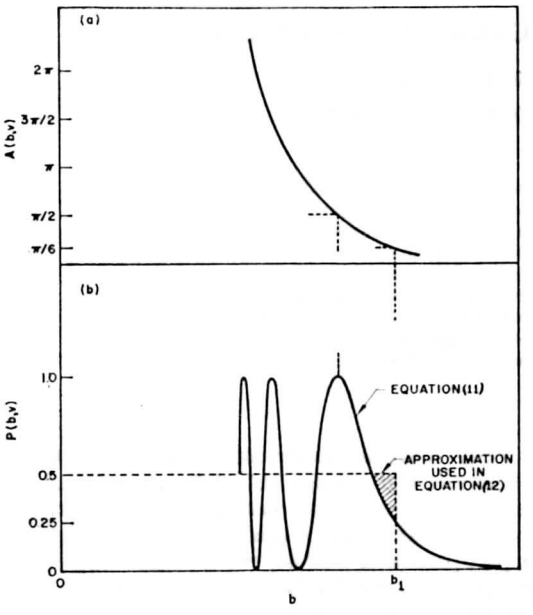

FIG. 1. (a) The function $A(b, v)$ that occurs in Eq. (11). (b) The function $P(b, v)=\sin^2[A(b, v)]$ showing the probability of charge exchange vs impact parameter at a fixed ion velocity. The approximation of Eq. (12) is shown by the dotted line.

velocity region is discussed only briefly in a separate section.

III. SYMMETRIC RESONANT CHARGE TRANSFER

The expression for the cross section for symmetric charge transfer in the "intermediate" velocity region has been derived independently by a number of authors. The final result is that the probability of charge transfer in a collision with velocity v and impact parameter b is given by[7,8]

$$P(b, v) = \sin^2\left[\int_{-\infty}^{+\infty} \frac{(E_a-E_s)dx}{2\hbar v}\right]. \quad (3)$$

This expression is derived from an analysis of the A_2^+ collision complex, formed from $A^+ + A$, as a one-electron problem. In other words, A is considered to be $(A^+ + e^-)$, and A^+ is a point center of positive charge. The result of this assumption is that the nonstationary state (which represents the collision) can be expressed in terms of symmetric and antisymmetric stationary states, with energies E_s and E_a, respectively. The cross section is then calculated from

$$\sigma(v) = 2\pi\int_0^\infty P(b, v)\, b db. \quad (4)$$

The calculation of σ for any substance depends only on (E_a-E_s) along the collision orbit x. Since (E_a-E_s) depends only on R, the internuclear separation of A^+ and A, and $R^2=x^2+b^2$, the determination of (E_a-E_s) vs R is the only unknown in the calculation. This quantity can only be calculated accurately from fundamental wave mechanics for H_2^+.[9] Wave-mechanical calculations for He_2^+ have also been made,[10] though they are not as accurate. These calculations of (E_a-E_s) have been used in Eqs. (3) and (4) for the processes[10,11]

$$H^+ + H \rightarrow H + H^+, \quad (5)$$

$$He^+ + He \rightarrow He + He^+, \quad (6)$$

and the results will be shown in Figs. 3(a) and (b) as curves A and M, respectively.

For more complex reactants, wave-mechanical calculations are too difficult. Several approaches, in terms of Slater orbitals,[3] hydrogenic orbitals,[8] and semi-empirical orbitals[12,13] have been proposed. We adopt the latter procedure. The one-electron wave function for $(A^+ + e^-)$ is chosen as[13]

$$\psi(r) = (\pi a_0^3)^{-\frac{1}{2}}(I/13.6)^{3/4}\exp[-(I/13.6)^{\frac{1}{2}}r/a_0], \quad (7)$$

in which a_0 is the Bohr radius, I is the ionization potential of A in electron volts, and r is the separation of A^+ from e^-. For $H^+(1s)$, $I=13.6$, and $\psi(r)$ reduces to the accurate function $a_0^{-\frac{3}{2}}\pi^{-\frac{1}{2}}\exp(-r/a_0)$. For atoms other than H, this expression is a gross approximation, especially when the outer electron is not in an s state. However it does roughly correlate the size of an orbital with the ionization potential, which is sufficient for our approximate calculations. For $R/a_0 \gg 1$ the (E_a-E_s) calculated for A_2^+ from the wave function in Eq. (7) is

$$(E_a-E_s) = 2I(R/a_0)\exp[-(I/13.6)^{\frac{1}{2}}R/a_0]. \quad (8)$$

For H_2^+, this reduces to the LCAO result,[8,13] $27.2(R/a_0)\exp(-R/a_0)$ eV. The complete characteristics of A_2^+ are thus expressed in terms of the ionization potential of A. While Eq. (8) gives the plausible result that a higher I gives rise to a smaller range interaction, one must not lose sight of the great oversimplification involved in this expression. Iovitsu and Pallas included an empirically adjusted parameter α in their exponent, which we omit because we wish to work on a completely *a priori* basis.

To obtain σ by applying Eq. (8) to Eqs. (3) and (4), one must evaluate the integral in

$$P(b, v) = \sin^2\int_{-\infty}^{+\infty}\left(\frac{I}{a_0\hbar v}\right)(x^2+b^2)^{\frac{1}{2}} \times \exp[-(I/13.6)^{\frac{1}{2}}(x^2+b^2)^{\frac{1}{2}}/a_0]dx. \quad (9)$$

[7] References 2–4 are but a few of the many available papers in this connection.

[8] D. Rapp and I. B. Ortenburger, J. Chem. Phys. **33**, 1230 (1960).

[9] D. R. Bates, K. Ledsham, and A. L. Stewart, Phil. Trans. Roy. Soc. **A246**, 215 (1953).

[10] B. L. Moiseitch, Proc. Phys. Soc. (London) **A69**, 653 (1956).

[11] T. J. M. Boyd and A. Dalgarno, Proc. Phys. Soc. (London) **A72**, 694 (1958).

[12] A. Dalgarno, Phil. Trans. Roy. Soc. **A250**, 426 (1958).

[13] I. Popescu Iovitsu and N. Ionescu-Pallas, Soviet Phys.—Tech. Phys. **4**, 781 (1960).

This integral has been evaluated by Dalgarno,[12] the result being

$$P(b, v) = \sin^2\left\{\frac{21b^2}{a_0\hbar v}\left[K_0(\gamma b/a_0) + \frac{K_1(\gamma b/a_0)}{(\gamma b/a_0)}\right]\right\} \quad (10)$$

in which $\gamma = (I/13.6)^{\frac{1}{2}}$, and K_0 and K_1 are Bessel functions of the second kind, of zero- and first-order, respectively. Since Eq. (8) is only a reasonable approximation for $(\gamma R/a_0) \gg 1$, Eq. (10) should only be applied in the range $(\gamma b/a_0) \gg 1$, for which the asymptotic forms of the Bessel functions[14] may be used. The result is

$$P(b, v) = \sin^2\left[\left(\frac{2\pi}{\gamma a_0}\right)^{\frac{1}{2}}\left(\frac{I}{\hbar v}\right)b^{\frac{1}{2}}\left(1+\frac{a_0}{\gamma b}\right)\exp\left(-\frac{\gamma b}{a_0}\right)\right]. \quad (11)$$

The form of the argument of the sine function in Eq. (11), to be denoted as $A(b, v)$, is shown in Fig. 1(a). The probability of charge transfer, $P(b, v) = \sin^2[A(b, v)]$ is shown in Fig. 1(b). The probability oscillates between 0 and 1 at small b, finally decaying to zero at large b. In the spirit of the approximate approach used in the present calculation, we replace this oscillating function by the constant value 0.5 from $b=0$ to the point b_1, where $P(b_1, v) = 0.25$. The choice of this point is somewhat arbitrary, but the dotted line in Fig. 1(b) representing the assumption made in the present choice shows it is roughly equivalent to approximating the "tail" of $P(b, v)$ by the shaded area. The cross section for charge exchange is then simply

$$\sigma = \tfrac{1}{2}\pi b_1^2. \quad (12)$$

To find b_1 we use the equality

$$A(b_1, v) = \left[\left(\frac{2\pi}{\gamma a_0}\right)^{\frac{1}{2}}\left(\frac{I}{\hbar v}\right)b_1^{\frac{1}{2}}\left(1+\frac{a_0}{\gamma b_1}\right)\exp\left(-\frac{\gamma b_1}{a_0}\right)\right] = \frac{\pi}{6}. \quad (13)$$

For $(\gamma b_1/a_0) \gg 1$, the variation of the exponential $\exp(-\gamma b_1/a_0)$ with b_1 in Eq. (13) is much greater than the variations of the pre-exponential term $b_1^{\frac{1}{2}}[1+(a_0/\gamma b_1)]$. To obtain the dependence of b_1 on v for limited ranges of v, one may replace the pre-exponential factors of b_1 by average values $\bar{b}_1$, and only seek the variation due to the exponential. Upon rearranging, the result is

$$\sigma^{\frac{1}{2}} = (\tfrac{1}{2}\pi)^{\frac{1}{2}}b_1 = -(\tfrac{1}{2}\pi)^{\frac{1}{2}}(a_0/\gamma)\ \ln v + (\tfrac{1}{2}\pi)^{\frac{1}{2}}(a_0/2\gamma) \times \ln\left[\frac{72\bar{b}_1^3}{\pi\gamma a_0}\left(\frac{I^2}{\hbar^2}\right)\left(1+\frac{a_0}{\gamma\bar{b}_1}\right)^2\right]. \quad (14)$$

This result has the well-known form[12,13]

$$\sigma^{\frac{1}{2}} = -k_1 \ln v + k_2 \quad (15)$$

which has been used for extrapolating charge-transfer data over velocity ranges.[13] It is noteworthy that over wide ranges of v, b_1 varies significantly, and one cannot choose an average $\bar{b}_1$ for the pre-exponential terms. The simple relation given in Eq. (15) is then not obeyed. For wide velocity ranges one can calculate σ vs v for any atom with only a knowledge of its ionization potential, by solving for b_1 in Eq. (14). Results of such a calculation are presented for a selection of atoms in Fig. 2 as a composite plot of $\sigma^{\frac{1}{2}}$ vs $\ln v$. The dependence of σ on I can be seen by comparing $\sigma^{\frac{1}{2}}$ in Fig. 2 with the ionization potentials listed in Table I.

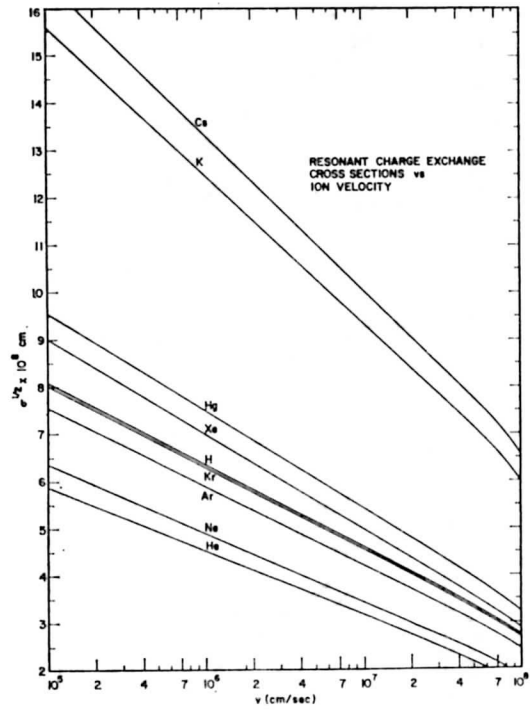

FIG. 2. Calculated cross sections for resonant charge exchange between monatomic ions and their parent gases. Interpolation can be made for other gases in terms of their ionization potentials (listed in Table I).

TABLE I. Ionization potentials used in preparation of Fig. 2.

Atom	I (eV)
He	24.6
Ne	21.6
Ar	15.8
Kr	14.0
H	13.6
Xe	12.1
Hg	10.4
K	4.1
Cs	3.9

[14] A. Erdelyi, W. Magnus, F. Oberhettinger, and F. G. Tricomi, *Higher Transcendental Functions*, Bateman Manuscript Project (McGraw-Hill Book Company, Inc., New York, 1954), Vol. I, p. 86.

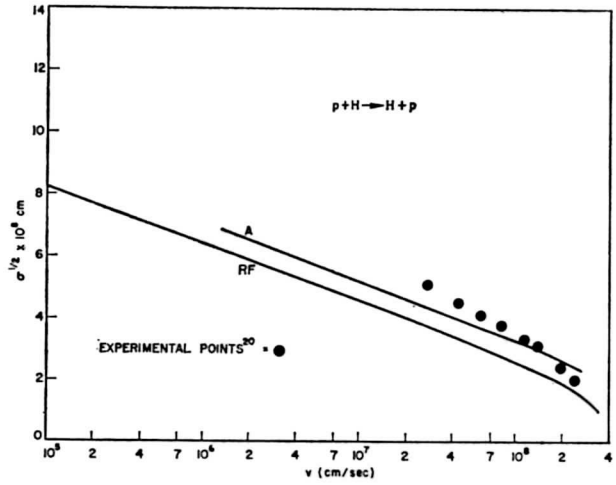
p+H→H+p
A
RF
EXPERIMENTAL POINTS[20]
σ^1/2 x 10^8 cm
v (cm/sec)

(a)

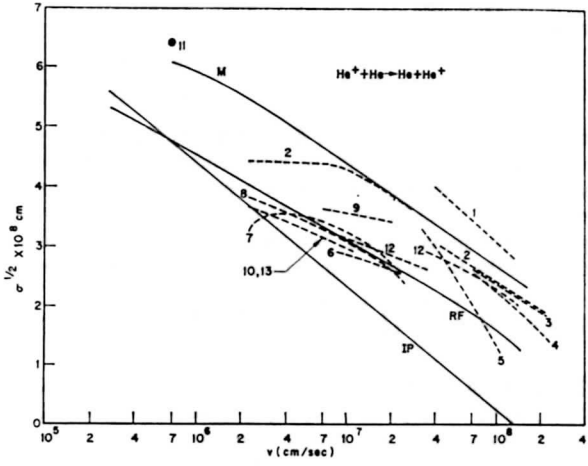
He⁺+He→He+He⁺
M
2
1
9
8
7
6
12
10,13
RF
IP
3
4
5
σ^1/2 X10^8 cm
v (cm/sec)

(b)

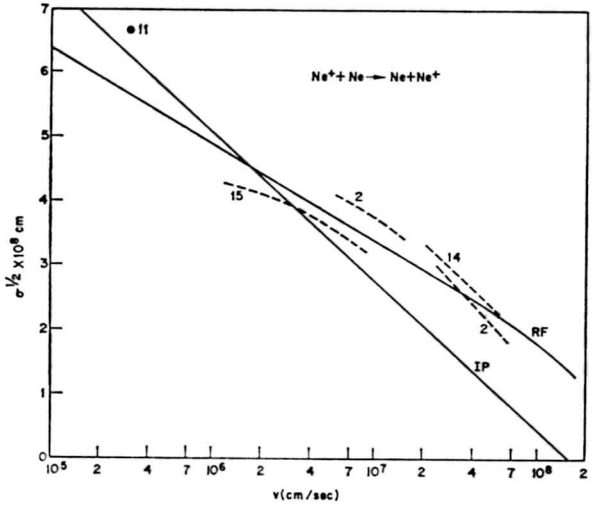
Ne⁺+Ne→Ne+Ne⁺
11
15
2
14
2'
RF
IP
σ^1/2 X10^8 cm
v(cm/sec)

(c)

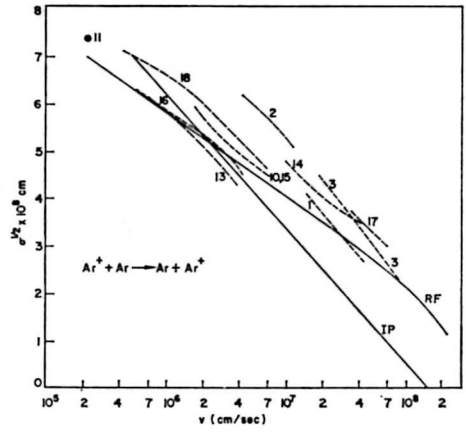
Ar⁺+Ar→Ar+Ar⁺
11
18
16
2
14
13
10,15
3
17
RF
IP
σ^1/2 x 10^8 cm
v (cm/sec)

(d)

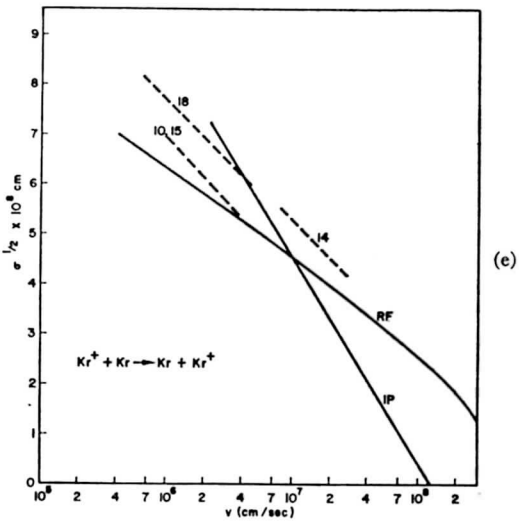
Kr⁺ + Kr→Kr + Kr⁺
18
10,15
14
RF
IP
σ^1/2 x 10^8 cm
v (cm/sec)

(e)

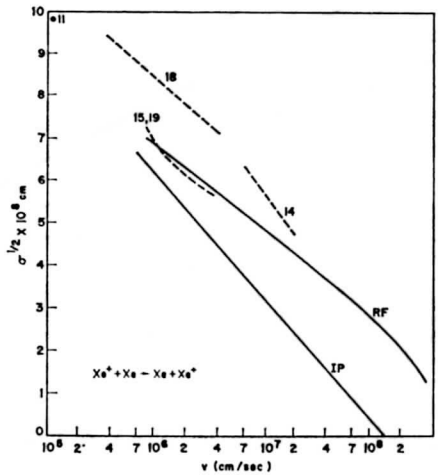
Xe⁺+Xe→Xe+Xe⁺
11
18
15,19
14
RF
IP
σ^1/2 X 10^8 cm
v (cm/sec)

(f)

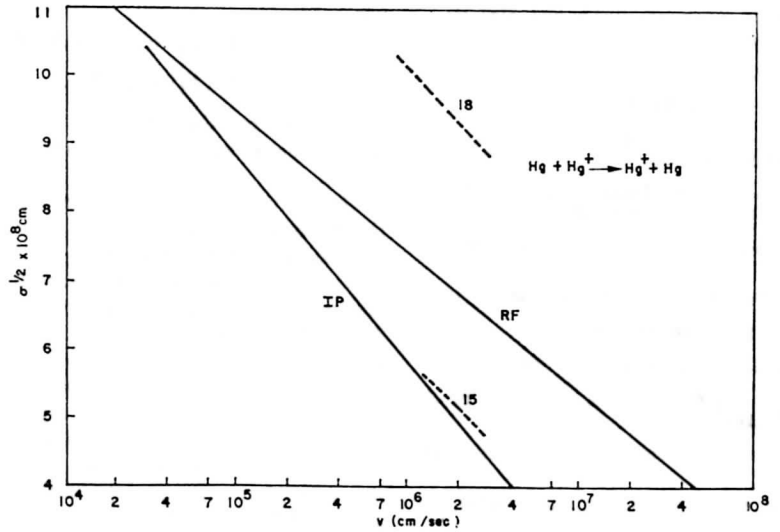

(g)

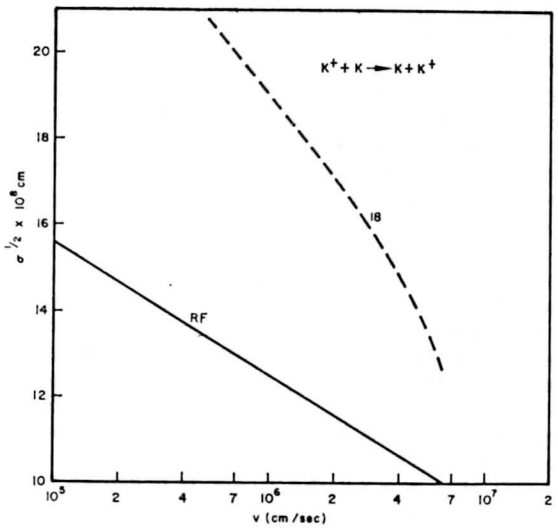

(h)

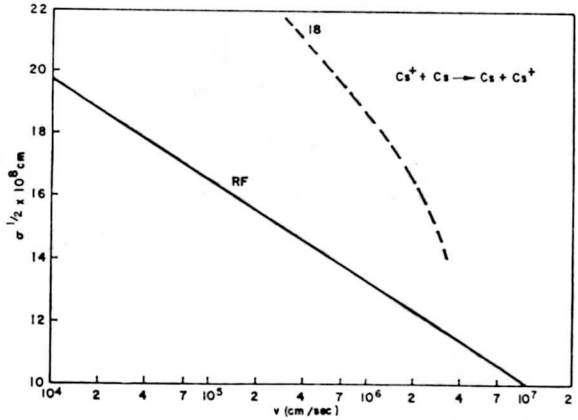

(i

FIG. 3(a)–(i) The calculated $\sigma(v)$ curves from Fig. 2, individually labeled "RF", are compared with available experimental references listed in Table II. Other theoretical calculations are presented in some cases (solid lines) and are labeled by letters according to the theoretical references in Table II.

Before comparing these calculations with the available experimental data, there is a further stipulation to be made. Equation (3) and the entire development leading to Fig. 2, are based upon a two-state approximation. That is, it is assumed that in a collision of an ion A^+ in its lowest state (i) with A in its lowest state (j), the collision complex A_2^+ may be treated analogously to H_2^+ which has gerade and ungerade states that go asymptotically to $\{A^+(i)+A(j)\}$. Nonadiabatic transitions to higher A_2^+ states resulting in products such as $\{A^+(k)+A(l)\}$ are neglected. Thus, only the reaction

$$A^+(i)+A(j)\rightarrow A(j)+A^+(i) \qquad (16)$$

is theoretically calculated, whereas actual experiments possibly involve charge exchange with excitation such as

$$A^+(i)+A(j)\rightarrow A(k)+A^+(l)+\Delta E, \qquad (17)$$

which though nonresonant, may have considerable cross sections at high energies (see Sec. IV). Furthermore, the initial ion beams used in experiments may

TABLE II. Reference for curves presented in Figs. 3(a)–(i).

(a) Experimental references

(1) J. P. Keene, Phil. Mag. **40**, 369 (1949).

(2) H. B. Gilbody and J. B. Hasted, Proc. Roy. Soc. (London) **A238**, 334 (1956).

(3) N. V. Fedorenko, V. V. Afrosimov and D. M. Kaminker, J. Tech. Phys. (U.S.S.R.) **26**, 1861 (1957).

(4) C. F. Stier and C. F. Barnett, Phys. Rev. **109**, 385 (1958).

(5) R. A. Smith, Proc. Cambridge Phil. Soc. **30**, 21 (1934)

(6) F. Wolf, Ann. Physik **30**, 21 (1937).

(7) A. Rostagni, Nuovo cimento **15**, 117 (1939).

(8) N. Dallaporta and G. Bonfiglioli, Comment. Pontif. Acad. Sci. **7**, 141 (1943).

(9) S. N. Ghosh and W. F. Sheridan, J. Chem. Phys. **26**, 480 (1957).

(10) J. B. Hasted, Proc. Roy. Soc. (London) **A205**, 421 (1951).

(11) B. Ziegler, Z. Physik **136**, 108 (1953).

(12) J. B. Hasted and J. B. H. Stedeford, Proc. Roy. Soc. (London) **A227**, 466 (1955).

(13) R. F. Potter, J. Chem. Phys. **22**, 974 (1954).

(14) I. P. Flaks and E. S. Solov'ev, Soviet Phys.—Tech. Phys. **3**, 564 (1958).

(15) J. A. Dillon, Jr., W. F. Sheridan, H. D. Edwards, and S. N. Ghosh, J. Chem. Phys. **23**, 776 (1955).

(16) W. H. Cramer, J. Chem. Phys. **30**, 641 (1959).

(17) P. R. Jones, F. B. Ziemba, H. A. Moses and E. Everhart, Phys. Rev. **113**, 182 (1959).

(18) R. M. Kushnir, B. M. Palyukh, and L. A. Sena, Bull. Acad. Sci. U.S.S.R., Phys. Ser. **23**, 995 (1959).

(19) S. N. Ghosh, *et al.*, Geophysical Research Paper No. 48, AirForce Cambridge Research Center, Bedford, Massachusetts.

(20) W. L. Fite, R. T. Brackman, and W. R. Snow, Phys. Rev. **112**, 1161 (1958).

(21) J. B. Hasted, Proc. Roy. Soc. (London) **A212**, 235 (1952).

(b) Theoretical references

(M) B. L. Moiseiwitsch, Proc. Phys. Soc. (London) **A69**, 653 (1956).

(A) T. J. M. Boyd and A. Dalgarno, Proc. Phys. Soc. (London) **A72**, 694 (1958).

(IP) I. Popescu-Iovitsu and N. Ionescu-Pallas, Soviet Phys. —Tech. Phys. **4**, 781 (1960).

contain excited states of A^+, which could react analogously to reactions (16) and (17), but involving other states. This is particularly true of the rare-gas ions from Ne^+ on up, where the spin-orbit interaction results in appreciable splitting in energy between the $P_{\frac{1}{2}}$ and $P_{\frac{3}{2}}$ states of the ion. For such a rare-gas ion system, the present calculations only account for reactions of the type

$$A^+(P_{\frac{1}{2}})+A \rightarrow A+A^+(P_{\frac{1}{2}}), \tag{18}$$

$$A^+(P_{\frac{3}{2}})+A \rightarrow A+A(P_{\frac{3}{2}}), \tag{19}$$

whereas the reactions in which $A^+(P_{\frac{1}{2}}) \leftrightarrows A^+(P_{\frac{3}{2}})$ may possibly be of considerable importance in some energy ranges.

The calculations shown in Fig. 2 are compared with the experimental cross sections, reaction by reaction, as solid curves RF in Figs. 3(a)–(i). Since it is difficult to select which data are most reliable, all available data are presented as dotted lines referenced according to Table II. In general the elementary theory described in this paper gives the correct qualitative behavior of the cross sections as functions of ion velocity. The calculations tend to lie below the experimental data, and this may be due to several reasons. One explanation is that Eq. (8) probably tends to underestimate the interaction, since it certainly underestimates the interaction for H_2^+[9] and He_2^+.[10] Use of more accurate interactions in these simple cases[10,11] leads to the cross-section curves A and M in Figs. 3(a) and (b), respectively. These curves lie above those based on Eq. (8) as the interaction. Contribution of reactions of type (17) would also lead to experimental cross sections larger than those calculated only for reaction (16). If one were assured that reaction (16) predominated in the experiments, one could work "backwards" and determine the interaction from the observed velocity dependence of the cross section.[15–17]

In a previous calculation,[13] an attempt to do this was made by the insertion of an empirically determined parameter "α" in the exponent of Eq. (8). Iovitsu and Ionescu-Pallas[13] used a wave-mechanical method which for "intermediate" velocities is analogous to the semi-classical procedure used in the present paper.[2,3] However, in their final result they obtained a cross section of the form given in Eq. (15) for all velocities. The proper result based on Eq. (8) as the interaction leads to Eq. (14), which does not produce the form given in Eq. (15) over wide velocity ranges. It is difficult to compare the two methods exactly, but it is apparent that they made an assumption which is analogous to setting $\bar{b}_1$ constant for all ion velocities. Furthermore, in obtaining the empirical parameter α, they made a trivial algebraic error which leads to serious numerical conflicts. On their graphs with ordinate labeled $\pi^{\frac{1}{2}}\sigma^{\frac{1}{2}}$, they apparently plotted their theoretical curve correctly, but plotted values of $\sigma^{\frac{1}{2}}$ for the high-energy experimental data. As a result, the data shown in their graphs should be multiplied by $\pi^{\frac{1}{2}}$, which would lead to a different value for their parameter α. Figures 3(a)–(f) show how their calculations, labeled "IP," fall

[15] E. A. Mason and J. T. Vanderslice, J. Chem. Phys. **29**, 361 (1958); **30**, 599 (1959).

[16] W. H. Cramer, and J. H. Simons, J. Chem. Phys. **26**, 1272 (1957).

[17] W. H. Cramer, J. Chem. Phys. **28**, 688 (1958).

below ours, labeled RF, at the higher energies because of this mistake.

The comparison made between theory and experiment in Figs. 3(a)–(i) leads to the general conclusion that most of the data apparently can be correlated in terms of a simple two-state theory, and that Fig. 2 is a useful result for rough predictions of atomic charge-transfer cross sections in the "intermediate" velocity range. For atoms other than those listed, one can interpolate in terms of their ionization potentials.

IV. ASYMMETRIC CHARGE TRANSFER (THE BASIC EQUATIONS)

The semiclassical treatment of asymmetric charge transfer in the intermediate velocity range has been discussed previously.[3,4,17] Procedures in terms of a two-state approximation analogous to symmetric charge transfer have been started. However the theory is not complete, and further discussion is required before a quantitative calculation can be attempted. In asymmetric charge transfer, further elaboration of statistical considerations, and of the approximate substitution of atomic orbitals for molecular orbitals is required. These considerations present no problems in the symmetric case. The purpose of the present section is to discuss three basic aspects of the theory of asymmetric charge transfer; statistical considerations, the approximate substitution of atomic orbitals for molecular orbitals in the expansion of the total wave function, and the relationship of the theory to the requirements of detailed balance. The actual calculation of cross sections from these general equations is left for Sec. V.

We first discuss the electronic states involved in the charge transfer process, and show the effects of the symmetries of these states. In the symmetric resonant process [Eq. (1)], even though there are two A_2^+ states involved in the collision there is only one asymptotic state at $R_{AA^+}=\infty$, $A^+ + A$. However, in the non-resonant reaction between particular electronic states

$$A^+(i)+B(j)\rightarrow A(k)+B^+(l), \qquad (20)$$

there are two different asymptotic states, $(A^+ + B)$ and $(A + B^+)$. Each of these are asymptotic forms of different electronic states of AB^+. Charge transfer requires an electronic transition from one electronic state to the other. Since charge transfer collisions in the "intermediate" velocity region involve relatively large impact parameters, we assume that angular momentum and spin are probably conserved in reaction (20). Thus, only transitions between states of AB^+ with identical symmetry are considered. One need, therefore, only consider the two electronic states of AB^+ with identical symmetry which go to $(A^+ + B)$ and $(A + B^+)$ as asymptotic forms. One thereby assumes allowed reactions analogous to that given by Eq. (20), but involving excited states of products such as

$$A^+(i)+B(j)\rightarrow A(m\neq k)+B^+(n\neq l), \qquad (21)$$

have such high values of $|\Delta E|$ that they are negligible. That is, if the electronic energy level of $\{A(m)+B^+(n)\}$ lies considerably above that of $\{A(k)+B^+(l)\}$, one may hope that the states of AB^+ for which they are asymptotic lie far enough apart in potential energy not to interact appreciably. This is what we mean by a "two-state approximation."

When $A^+(i)$ and $B(j)$ collide, several states of AB^+ may be formed. The probability that any state may be formed is proportional to its statistical weight. Only those states with identical symmetry with

$$\{A(k)+B^+(l)\}$$

can produce charge transfer according to reaction (20), so this reaction is forbidden by symmetry considerations in a certain fraction of the collisions. The fraction of collisions that produce AB^+ states which allow charge transfer will be denoted as f, the statistical weight factor. The ratio f_1/f_2 for forward and backward reactions in Eq. (20) is the pre-exponential factor of the equilibrium constant for the reactions.[18] In comparing theoretical cross sections with experiment, one must multiply the calculated cross section based on the two-state approximation by f before comparison with experiment. In a previous paper,[8] a brief application of these symmetry principles was given for the charge transfer reactions of N^+ and O^+ with H. A more easily visualized example is provided by the reactions

$$He^+(^2S)+H(^2S)\leftrightarrows He(^1S)+H^+. \qquad (22)$$

There are two HeH^+ states which go asymptotically to $\{He^+(^2S)+H(^2S)\}$, and they have symmetries $^3\Sigma$ and $^1\Sigma$. There is one state which goes to $\{He(^1S)+H^+\}$, which is $^1\Sigma$. Considering the backward reaction, a collision between $He(^1S)$ and H^+, can only produce a $^1\Sigma$ transient state of HeH^+, and charge transfer must occur to the other $^1\Sigma$ state of HeH^+ which goes asymptotically to $\{He^+(^2S)+H(^2S)\}$. Nevertheless, the statistical factor f_2 for the backward reaction is unity because all collisions can produce reaction. In the forward reaction, $\frac{1}{4}$ of the collisions between $He^+(^2S)$ and $H(^2S)$ produce $^1\Sigma$ states which can lead to charge transfer, whereas $\frac{3}{4}$ of the collisions produce $^3\Sigma$ states which cannot lead to charge transfer. Thus f_1 for the forward reaction is $\frac{1}{4}$.

Bates and Lynn[19] have pointed out that there are two ways of making the "two-state approximation," involving expansions of the total wave function in terms of either atomic or molecular orbitals. In each case the expansion is held to two terms, corresponding to reactants and products, the respective time-dependent coefficients determining the probability of finding the system in each state. Since one does start out with reactants before collision, the initial condition is that

[18] The equilibrium constant for reaction (21) is $f_1/f_2 e^{-\Delta E/RT}$, where in more usual terms $f_1/f_2=(g_A g_B{}^+/g_A{}^+ g_B)$, and the g's are statistical weights of the atoms.

[19] D. R. Bates and N. Lynn, Proc. Roy. Soc. (London) **A253**, 141 (1959).

one coefficient is unity and the other zero at $t=-\infty$. The problem is then to calculate the other coefficient after collision, at $t=+\infty$, from the time-dependent Schroedinger equation. In symmetric resonant charge transfer, similar expansions are used. It may be shown[2,8,20] that use of the molecular wave functions leads to Eq. (3), whereas the atomic orbitals lead to Eq. (3) with (E_a-E_e) replaced by the LCAO approximation to this quantity. The connection between the molecular and atomic orbital approaches in asymmetric charge transfer is not so easily obtained.

The proper approach involves writing the total wave function as a linear combination of molecular orbitals of AB^+ formed in the collision of A^+ with

$$\Psi=c_A(t)\Phi_A^{(AB+)}(R)\exp[-iE_A^{(AB+)}(R)t/\hbar]+c_B(t)\Phi_B^{(AB+)}(R)\exp[-iE_B^{(AB+)}(R)t/\hbar], \quad (23)$$

in which $\Phi_i^{(AB+)}(R)$ is the molecular orbital of AB^+ which goes to ϕ_i as $R\rightarrow\infty$, and $E_i^{(AB+)}(R)$ is the energy of this state (which goes to ϵ_i as $R\rightarrow\infty$). Since Eq. (23) leads to differential equations difficult to solve, we follow Gurnee and Magee,[3] and utilize the zeroth-order approximation of replacing the molecular wave functions and energies by atomic orbitals and atomic energies. This approximation is only reasonable at large internuclear separations.

The asymmetric charge-transfer process Eq. (20), is written as

$$A^+ + (B^+ + e^-) \rightarrow (A^+ + e^-) + B^+. \quad (24)$$

In this simple picture, there is a single valence electron which can be attached to either nucleus, A^+ or B^+. The total wave function for the electron in the combined field of A^+ and B^+ is written as

$$\Psi=c_A(t)\phi_A(r_A)\exp(-i\omega_A t)+c_B(t)\phi_B(r_B)\exp(-i\omega_B t), \quad (25)$$

where the c's are time-dependent coefficients of the expansion, ϕ_A and ϕ_B are atomic orbitals for the electron on nuclei A^+ and B^+, r_A and r_B are the distances of the electron from A^+ and B^+, $\omega=\epsilon/\hbar$, and ϵ_A and ϵ_B are the energies (ionization potentials) of A and B in states ϕ_A and ϕ_B, respectively. These states are solutions of the atomic Schrödinger equations

$$[(-\hbar^2/2m_e)\nabla^2+V_j(r_j)]\phi_j=\epsilon_j\phi_j, \quad (26)$$

in which j can either be A or B, and $V_A(r_A)$ is the effective potential binding e^- to A^+. The time-dependent wave equation for the electron in the presence of A^+ and B^+ is

$$[(-\hbar^2/2m_e)\nabla^2+V_A(r_A)+V_B(r_B)]\Psi=\hbar i(\partial\Psi/\partial t). \quad (27)$$

The collision coordinates are the same as those discussed in Sec. I for symmetric charge transfer. The classical trajectory $x=vt$ relates the relative motion of A^+ and B^+, and for any value of $x=(R^2-b^2)^{\frac{1}{2}}$, r_A and r_B are not independent. Use of Eq. (25) for Ψ in Eq. (27) leads to an equation in c_A, $\dot{c}_A$, c_B and $\dot{c}_B$. This equation relates the coefficients c_A and c_B during the collision under the action of the perturbation V_A (assuming the electron was initially on B^+). When this equation is multiplied alternately by ϕ_A and ϕ_B, and integrated over-all space, two coupled differential (with respect to time) equations in c_A and c_B are obtained

$$[(V_B)_{AA}/\hbar]c_A+[(V_A)_{AB}/\hbar]\exp(-i\omega t)c_B=i[\dot{c}_A+F\exp(-i\omega t)\dot{c}_B], \quad (28)$$

$$[(V_B)_{BA}/\hbar]\exp(i\omega t)c_A+[(V_A)_{BB}/\hbar]c_B=i[F\exp(i\omega t)\dot{c}_A+\dot{c}_B]. \quad (29)$$

In these equations, $\omega=\omega_B-\omega_A$, and integrals are defined as

$$(V_j)_{mn}=\int\phi_m V_j(r_j)\phi_n d\tau,$$

$$F=\int\phi_A\phi_B d\tau.$$

These integrals are functions only of R, the internuclear separation of A^+ and B^+, and from the classical collision trajectory are therefore functions only of t. Since the probabilities of locating the electron on nuclei A^+ and B^+ are $|c_A|^2$ and $|c_B|^2$, respectively, the initial condition is taken as

$$c_A(-\infty)=0,$$

$$c_B(-\infty)=1,$$

which locates the electron on nucleus B^+ before collision. The probability of finding the electron on nucleus A^+ after collision $|c_A(+\infty)|^2$ multiplied by the statistical weight factor f, is the charge transfer probability $P(b,v)$ in a collision of velocity v and impact parameter b.

Equations (28) and (29) may be simplified to

$$i\dot{c}_B=\kappa_1(t)\exp(i\omega t)c_A+\eta_1(t)c_B, \quad (30)$$

$$i\dot{c}_A=\eta_2(t)c_A+\kappa_2(t)\exp(-i\omega t)c_B, \quad (31)$$

in which the κ's and η's are groupings of perturbation integrals divided by $\hbar$:

$$\kappa_1=\left[\frac{(V_B)_{BA}-F(V_B)_{AA}}{(1-F^2)\hbar}\right], \qquad \kappa_2=\left[\frac{(V_A)_{AB}-F(V_A)_{BB}}{(1-F^2)\hbar}\right]$$

$$\eta_1=\left[\frac{(V_A)_{BB}-F(V_A)_{AB}}{(1-F^2)\hbar}\right], \qquad \eta_2=\left[\frac{(V_B)_{AA}-F(V_B)_{AB}}{(1-F^2)\hbar}\right]$$

By defining new coefficients, a_A and a_B, such that

$$c_B=a_B\exp\left(-i\int_{-\infty}^{t}\eta_1 dt'\right), \qquad c_A=a_A\exp\left(-i\int_{-\infty}^{t}\eta_2 dt'\right)$$

[20] T. Holstein, J. Phys. Chem. **56**, 832 (1952).

Eqs. (30) and (31) are further simplified to

$$i\dot{a}_B = \kappa_1(t)\ \exp(i\Omega t)\, a_A, \tag{32}$$

$$i\dot{a}_A = \kappa_2(t)\ \exp(-i\Omega t)\, a_B, \tag{33}$$

in which

$$\Omega t = \omega t + \int_{-\infty}^{t} (\eta_1 - \eta_2)\, dt'. \tag{34}$$

Since $|a_A|^2 = |c_A|^2$, the probability of charge transfer is $f|a_A(+\infty)|^2$.

The relationship between the quantities κ_1, κ_2, and Ω, and the potential energy curves of the molecular AB^+ states (which go asymptotically to reactants and products) is undoubtedly complex. In symmetric resonant charge transfer, the atomic orbital approach leads to equations of the form given in Eqs. (32) and (33), except that[8] $\omega = \eta_1 - \eta_2 = 0$ and $\kappa_1 = \kappa_2 = (E_a - E_s)$. The differential equations may then be solved exactly[3] to yield Eq. (3), with $P(b, v) = |a_A(+\infty)|^2$, and $t = x/v$. In the asymmetric process, a critical examination is required to find any such relationships.

For our present purpose of calculating cross sections we need only compute the integrals in κ_1, κ_2, and Ω without considering their relationship to the potential curves. Since Eq. (25) is only justifiable as the total wave function at large impact parameters, the atomic orbitals in Eq. (7) for ϕ_A and ϕ_B are used. One can show[21] in the resonant case for $\phi_A = \phi_B$ that such orbitals lead to the result that at large R/a_0, integrals of the type $(V_i)_{jk}$ where $(j \neq k)$ are proportional to $R\exp(-\gamma R/a_0)$, integrals of the type $(V_i)_{jj}$ are proportional to $\exp(-2\gamma R/a_0)$, and F is proportional to $R^2\exp(-\gamma R/a_0)$. In the nonresonant case, use of Eq. (7) with a different value for I for each atom leads to more involved integrals. Some lengthy calculations lead to the conclusion that $\kappa_2 \approx (V_A)_{AB}$, $\kappa_1 \approx (V_B)_{BA}$, and $\kappa \gg \eta$. Therefore $\kappa_1(t)$ and $\kappa_2(t)$ have the same type of behavior as in the resonant case. One may show that use of the orbitals in Eq. (7) also leads to the conclusion that for a very near-resonance in which $|\omega_1 - \omega_2| \ll (\omega_1 \text{ or } \omega_2)$, $|\eta_1 - \eta_2|$ is also small.[22] One may also show that in the present approach $|\eta_1 - \eta_2| \ll |\omega|$ for $R/a_0 \gg 1$, so that the approximation $\Omega \cong \omega$ is justified in the present approximate calculation.[23]

There is one further point which requires consideration before we attempt to solve Eqs. (32) and (33) subject to the assumptions made in the previous paragraphs. The principle of detailed balance requires that in reaction (20) for a given b and v, $P_1(b, v)$ in the forward direction is related to $P_2(b, v)$ in the reverse direction by

$$P_1(b, v)/P_2(b, v) = f_1/f_2. \tag{34}$$

Since f_1 and f_2 enter our calculation because of statistical considerations [i.e., $P_1(b, v) = f_1|a_A(\infty)|^2$], we are led to the following conclusion: Starting with $\{A^+ + B\}$, [i.e., $a_A(-\infty) = 0$, $a_B(-\infty) = 1$], the $|a_A(\infty)|^2$ for charge transfer to $\{A + B^+\}$ should be the same as $|a_B(\infty)|$ for the reverse process [i.e., $a_A(-\infty) = 1$, $a_B(-\infty) = 0$]. Equations (32) and (33) do not satisfy this requirement unless $\kappa_1 = \kappa_2$. In the present treatment $\kappa_1 \neq \kappa_2$ because[8]

$$(V_B)_{AB} - (V_A)_{BA} = (\epsilon_A - \epsilon_B)F. \tag{35}$$

This reflects the fact that Eq. (25) only approximates the true total wave function. The particular choice made in Eq. (25) becomes more inadequate for larger nonresonances $(\epsilon_A - \epsilon_B)$. The reason for this is that one should really use Eq. (23) for the wave function of the collision complex AB^+. Since $\Phi_A^{(AB+)}(R)$ and $\Phi_B^{(AB+)}(R)$ are mutually orthogonal, and are eigenfunctions of the total Hamiltonian operator [left side of Eq. (27)], the choice of Eq. (23) in terms of molecular orbitals leads to differential equations which do satisfy detailed balance. Equation (25) is a "zeroth-order" approximation in which the asymptotic forms of Φ and E are used for finite R. The functions ϕ_A, ϕ_B are not orthogonal, except at $R = \infty$. It is this nonorthogonality which leads to $\kappa_1 \neq \kappa_2$. One may now ask what credence can be attached to a theory which does not satisfy detailed balance. The answer to this question lies in the behavior of $\Phi_i^{(AB+)}(R)$, $(i = A, B)$. At large R, the use of ϕ_i instead of Φ_i is a good approximation, and F in Eq. (35) is small. The discrepancy between κ_1 and κ_2 is then small. One may therefore be assured that the calculated $P(b, v)$ is a reasonable approximation at large b. However, since one must use Eq. (4) for σ, $P(b, v)$ has to be calculated for small b also. When the contribution to the integrand in Eq. (4) is relatively small for small b, the theory is most adequate. Thus, the theory works best when σ is large. In our calculations we utilize Eqs. (25), (32), and (33), but with an appropriate average κ used for both κ_1 and κ_2. In some calculations the important range of b in Eq. (4) is small enough that the present treatment is not strictly applicable.[24] Nevertheless reasonable qualitative agreement with experiment is often found from this simple approach.

Keeping in mind the discussion given in the previous

[21] L. Pauling and E. B. Wilson, Jr., *Introduction to Quantum Mechanics* (McGraw-Hill Book Company, Inc., New York, 1935), pp. 138–139.

[22] In the limit $\omega_1 = \omega_2$, $\eta_1 - \eta_2 = 0$ by this assumption. However, use of more realistic orbitals would lead to $\eta_1 - \eta_2 \neq 0$ when A and B are different even though $\omega_1 = \omega_2$. This case of "accidental resonance" is important in the reaction $O^+(^4S) + H(^2S) \rightarrow O(^3P) + H^+$ for which $\omega_1 - \omega_2$ is very small.[8,19] The contribution of $\eta_1 - \eta_2$ to Ω in such a process is difficult to ascertain accurately. At very large impact parameters $\Omega \cong \omega$ since $\eta_1 - \eta_2 \rightarrow 0$ as $b \rightarrow \infty$. Whether $\eta_1 - \eta_2$ is still negligible at the finite impact parameters involved in charge transfer, is subject to question.[19] In our approximate calculation we put $\Omega = \omega$ for all ω and b.

[23] Bates and Lynn[19] have pointed out that in processes of the type

$$A^+ + B^+ \rightarrow A^{++} + B,$$

$\eta_1 - \eta_2$ may be very large compared to ω, leading to $\Omega \neq \omega$. We do not consider such processes in this paper.

[24] In general, the smaller the nonresonance, and the higher the ion velocity, the better the present theory should be.

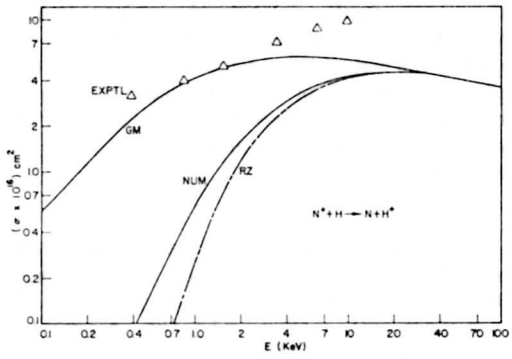

FIG. 4. Comparison of approximations of Gurnee and Magee[3] (GM) and Rosen and Zener[27] (RZ) with exact machine solution (NUM) of coupled equations for charge exchange. The data and the (GM) curve are taken from reference 8.

paragraph, we use the modified equations

$$iv(da_B/dx) = \bar{\kappa}(x/v)\, \exp(i\omega x/v)\, a_A, \qquad (37)$$

$$iv(da_A/dx) = \bar{\kappa}(x/v)\, \exp(-i\omega x/v)\, a_B, \qquad (38)$$

with $\bar{\kappa}$ an appropriate mean of κ_1 and κ_2, $a_A(-\infty)=0$, $a_B(-\infty)=1$, and $P(b, v)=f\,|\,a_A(+\infty)\,|^2$. Before attempting any quantitative calculations, we shall briefly discuss the qualitative features of Eqs. (37) and (38), and the $P(b, v)$ and σ calculated therefrom. The function $[\bar{\kappa}(x/v)/v]$ is just like the corresponding term in symmetric resonant charge transfer [i.e., the integrand in Eq. (9), with I replaced by an appropriate mean of I_A and I_B]. It is seen that the particular averaging process chosen is not as important as the value of ω, so that it suffices to say that whether one uses I_A, I_B, or some mean value, the dependence of σ on v is mainly determined by ω, except in very large nonresonances.

The main point is that $\bar{\kappa}(x/v)$ is a "bell-shaped" curve with a finite maximum at $x=0$, and which goes exponentially to zero at $x=\pm\infty$. This is the interaction causing charge transfer. For very small values of ω/v, the imaginary exponential terms in Eqs. (37) and (38) remain essentially at unity over the entire range of x for which κ is appreciable. Under this condition, the exponential terms may be set equal to unity and Eqs. (37) and (38) become identical to the equations obtained in the symmetric resonant case, the solution being Eq. (3) with (E_a-E_s) replaced by $\bar{\kappa}$. For a given ω, at high enough v that $(\omega x/v)$ is small, the behavior of $\sigma(v)$ is then similar to $\sigma(v)$ for symmetric resonant charge transfer (with an effective ionization potential somewhere between I_A and I_B), namely Eq. (14). In this velocity range, σ increases with decreasing velocity because there is more time available in the collision for an electronic transition to occur, and $\omega x/v$ is small enough that the transition is easily facilitated in proportion to the interaction $\bar{\kappa}$. At lower velocities the situation is somewhat different. Consider the case of a very large impact parameter for which the interaction $\bar{\kappa}$ is weak, and the transition probability is small. One may then put $a_B(x)\approx 1$ for all x, and calculate the perturbation approximation

$$|\,a_A(\infty)\,|^2 \cong \left|\frac{1}{v}\int_{-\infty}^{\infty}\bar{\kappa}\left(\frac{x}{v}\right)\cos\left(\frac{\omega x}{v}\right)dx\right|^2 \qquad (39)$$

in which $\exp(-i\omega x/v)$ has been replaced by $\cos(\omega x/v)$ since $\bar{\kappa}$ is an even function of x. The function $\bar{\kappa}$ has an effective width in x of the order of several atomic dimensions (i.e., several Bohr radii). Let a be such a dimension characterizing the range of $\bar{\kappa}$ in x.[25] Then as the ion velocity is reduced to the point where $(\omega a/v)$ becomes of the order of unity, the oscillations of $\cos(\omega x/v)$ begin to severely reduce $|\,a_A(\infty)\,|^2$, despite the pre-integral factor of $1/v$ acting weakly in the opposite direction. At lower velocities where $\omega a/v \gg 1$, $|\,a_A(\infty)\,|^2$ falls off rapidly with decreasing v. Thus, in between these velocity extremes, at some velocity near where one oscillation occurs between $x=-a$ and $x=+a$, a maximum charge transfer probability is obtained at large impact parameters. This determines the condition that the maximum cross section is obtained when

$$\omega a/V = a\,|\,\Delta E\,|\,/\hbar v \approx 1, \qquad (40)$$

which is in accord with the qualitative "near-adiabatic" theory proposed by Massey.[26]

V. ASYMMETRIC CHARGE TRANSFER (APPLICATIONS)

In any nonresonant charge transfer process, Eqs. (37) and (38) must be solved to obtain $P(b, v)$. Rosen and Zener[27] have solved them for the special case where $\bar{\kappa}$ is of the form $k_1\,\mathrm{sech}(k_2 x)$. They have proposed that the general form of the solution might be

$$a_A(+\infty)_{RZ}{}^2 = \left(\sin^2\int_{-\infty}^{\infty}\bar{\kappa}dt\right)\left(\int_{-\infty}^{\infty}\bar{\kappa}\cos\omega t dt\right)^2 \Big/ \left(\int_{-\infty}^{\infty}\bar{\kappa}dt\right)^2. \qquad (41)$$

Gurnee and Magee,[3] unaware of the paper by Rosen and Zener,[27] proposed a general solution of the form

$$|\,a_A(+\infty)\,|_{GM}{}^2 = \sin^2\int_{-\infty}^{\infty}\bar{\kappa}\cos\omega t dt. \qquad (42)$$

Bates and Lynn[17] pointed out that, since Eq. (42) does not work in the special case of $\bar{\kappa}=k_1\,\mathrm{sech}(k_2 x)$, it could not be the correct general solution. Skinner[28] did some numerical calculations for specific (b, v) combinations to show that Eq. (41) is also not a general solution for all $\bar{\kappa}$. However, it is difficult to ascertain

[25] A recent examination of the available data in terms of this conclusion leads to a "best" value of about 7 Å for a. [J. B. Hasted and A. R. Lee, University College, London (personal communication of a preprint to be published)].

[26] H. S. W. Massey, Rept. Progr. Phys. **12**, 248 (1949).

[27] N. Rosen and C. Zener, Phys. Rev. **40**, 502 (1932).

[28] B. G. Skinner, Proc. Phys. Soc. (London) **A77**, 551 (1961).

from this work just how valid the approximations of Eqs. (41) and (42) are.[29] In a previous calculation,[8] $\sigma(v)$ was calculated for

$$N^+ + H \rightarrow N + H^+ \tag{43}$$

using the (poor) approximation of Eq. (42). We have used the same $\bar{\kappa}$ of this previous work in two new calculations, one utilizing Eq. (41), and the other a numerical integration of Eqs. (37) and (38) on a digital computer. The results are shown in Fig. 4. It can be seen that above the velocity corresponding to the maximum σ, all three methods coincide. At lower velocities Eq. (41) is a much better approximation than Eq. (42). The details are not given here, but it may be shown that the best procedure is to fit the actual function $\bar{\kappa}$ in any example to a $k_1 \operatorname{sech}(k_2 x)$ curve, and then use the correct solution, Eq. (41). This procedure has been adopted in the present paper since in practice $\bar{\kappa}$ can only be estimated very roughly.

In the present calculation we have made assumptions leading to

$$\bar{\kappa}_1 = (I/a_0\hbar)\,(x^2+b^2)^{\frac{1}{2}} \exp\{-\gamma(x^2+b^2)^{\frac{1}{2}}/a_0\}, \tag{44}$$

with I some suitable mean between I_A and I_B. In order to fit this to

$$\bar{\kappa}_2 = k_1 \operatorname{sech}(k_2 x), \tag{45}$$

two conditions must be made. We make the reasonable (but arbitrary) choice: $\bar{\kappa}_1(0) = \bar{\kappa}_2(0)$, and

$$\int_{-\infty}^{\infty} \bar{\kappa}_1 dx = \int_{-\infty}^{\infty} \bar{\kappa}_2 dx.$$

The constants k_1 and k_2 may then be determined, leading to

$$k_1 = (I/a_0^2\hbar)\, b \exp(-\gamma b/a_0) \tag{46a}$$

$$k_2 = \pi\{2b \exp(\gamma b/a_0)[K_0(\gamma b/a_0) + K_1(\gamma b/a_0)/(\gamma b/a_0)]\}^{-1}. \tag{46b}$$

The solution to Eqs. (37) and (38) for $\bar{\kappa} = \bar{\kappa}_2$ is

$$|\, a_A(\infty)\,|^2 = \sin^2(\pi k_1/v k_2 a_0)\, \operatorname{sech}^2(\pi\omega/2vk_2). \tag{47}$$

It may be seen that this, when combined with Eqs. (46a) and (46b), leads to

$$P_\omega(b, v) = f P_0(b, v)\, \operatorname{sech}^2[(\omega a_0/\gamma v) F(\gamma b/a_0)], \tag{48}$$

in which f is the statistical factor mentioned in Sec. IV, $P_0(b, v)$ is the probability given by Eq. (10), and

$$F(\gamma b/a_0) = (\gamma b/a_0) \exp(\gamma b/a_0) \times\{K_0(\gamma b/a_0) + K_1(\gamma b/a_0)/(\gamma b/a_0)\}. \tag{49}$$

For $b/a_0 \gg 1$, the asymptotic forms of the Bessel functions may be used,[14] giving

$$F(\gamma b/a_0) \cong (\pi\gamma b/2a_0)^{\frac{1}{2}}. \tag{50}$$

For a given $(\omega/\gamma v)$, the sech function in Eq. (48) should become "broader" in b for smaller b. Since $[F(\gamma b/a_0)]^{-1}$ determines the "breadth" of the sech function, we make the (crude) assumption that the asymptotic form Eq. (50) holds for all b. This is reasonable despite the fact that Eq. (49) goes to ∞ at $b=0$, because Eq. (49) is only valid at large b. For example, at $\gamma b/a_0 < 1$, $\bar{\kappa}_1$ cannot even be fitted to $\bar{\kappa}_2$, because $\bar{\kappa}_1$ has a minimum, whereas $\bar{\kappa}_2$ has a maximum. The assumption that Eq. (50) can be used when $1 > \gamma b/a_0$, while poor, only leads to dubious cross sections when the region $1 > \gamma b/a_0 > 0$ contributes greatly to the integrand in Eq. (4). We therefore have the result

$$P_\omega(b, v) = f P_0(b, v)\, \operatorname{sech}^2[(\omega/v)\,(a_0\pi b/2\gamma)^{\frac{1}{2}}]. \tag{51}$$

To obtain σ from the integral in Eq. (4), consider the diagrams shown in Fig. 5. At very high velocities such that the adiabatic parameter $p \ll 1$, the sech function is essentially unity (curve A) over the important range of $P_0(b, v)$. Thus σ is simply f multiplied by the value calculated from Eq. (14). At velocities leading to $p \approx 1$ (curve B), one can replace $P_0(b, v)$ by $\frac{1}{2}$ from $0 < b < b_1$, and by 0 for $b > b_1$. The choice of b_1 is made as the point [30] where

$$\operatorname{sech}^2[(\omega/v)\,(a_0\pi b_1/2\gamma)^{\frac{1}{2}}] = 4P_0(b_1, v). \tag{52}$$

The cross section is then

$$\sigma(v) = \tfrac{1}{2} f \int_0^{b_1} \operatorname{sech}^2[(\omega/v)\,(a_0\pi b/2\gamma)^{\frac{1}{2}}]\, 2\pi b db. \tag{53}$$

For very low velocities where $p \gg 1$ (curve C), the upper limit of Eq. (53) may be set equal to ∞, and

$$\sigma(v) = (2\pi/\alpha^4) \int_0^{\infty} (\operatorname{sech}^2 u)\, u^3 du = \tfrac{2}{3}(1.202)\,(2\pi/\alpha^4), \tag{54}$$

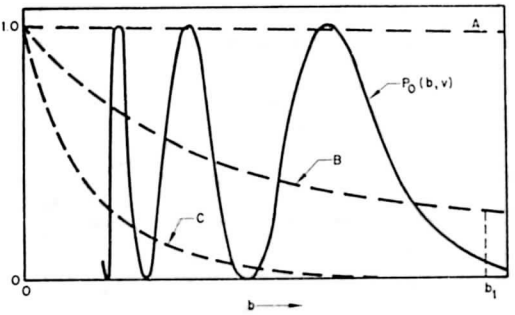

FIG. 5. Functions of importance in Eq. (51). $P_0(b, v)$ is that obtained from Eq. (11) in the resonant case. Curves A, B, and C are the function $\operatorname{sech}^2[(\omega/v)\,(a_0\pi b/2\gamma)^{\frac{1}{2}}]$ for successively higher (ω/v). Point b_1 is determined by the condition that the sech^2 function is four times $P_0(b_1, v)$.

[29] The various functions $|\, a_A(\infty)\,|^2$ oscillate with b with different frequencies, so that comparison at identical (b, v) combinations is not as meaningful as a comparison of the integrals obtained from Eq. (4).

[30] See the discussion immediately following Eq. (11).

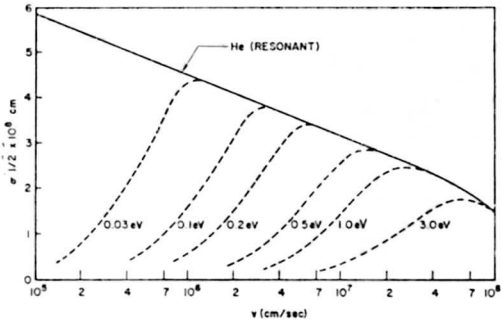

(a)

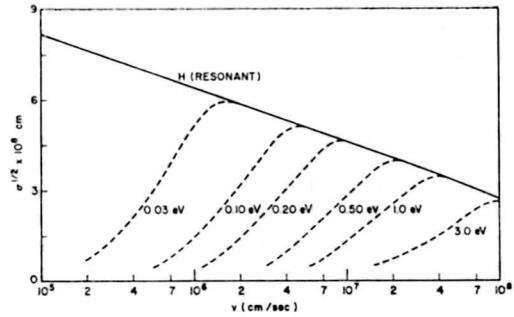

(b)

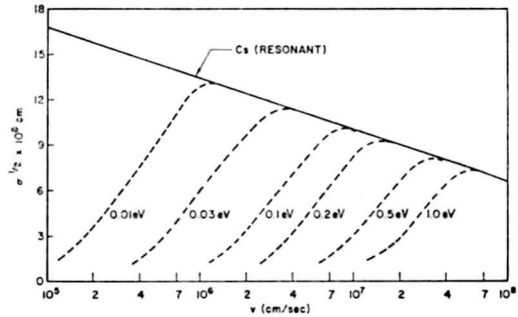

(c)

FIG. 6. Calculated $\sigma(v)$ for various ΔE in sets of processes having the same γ. (a), (b), (c) are for γ's of γ_{He}, γ_H, and γ_{Cs}, respectively. Note that in each case the nonresonant $\sigma(v)$ curves approach the corresponding resonant curve at high enough velocities that the adiabatic parameter $p=[(\Delta E)\ a/\hbar v]\ll 1$. The dependence of $\sigma(v)$ on ΔE is much more critical than the dependence on γ. For processes in which the ΔE is large, the choice of an effective γ becomes dubious, but a value close to the lower of the two atomic γ's seems more appropriate [see the discussion in the paragraph preceding Eq. (34)].

in which $\alpha=[(\pi a_0/2\gamma)^{\frac{1}{2}}(\omega/v)]$. Thus at low velocities,

$$\sigma \cong \frac{9(1.202)}{\pi}\frac{\gamma^2 v^4}{a_0^2\omega^4}. \tag{55}$$

We must point out that Eq. (55) is a very crude result for two reasons. First, the region of b contributing to the integral in Eq. (4) is small at low velocities, so that the use of Eq. (50) for all b is not justified. Secondly, the qualitative form of the result (i.e., $\sigma \approx v^4$) is very sensitive to assumptions made about the R dependence of $\tilde{\kappa}$. It is only by utilizing a sech function with Eq. (50) that we get the present result. Thus, Eq. (55) should only be used for order-of-magnitude calculations, and one should not seriously expect a plot of experimental σ vs v^4 to be linear.

The general result given in Eq. (53) shows σ to depend on I (through γ)[31] and ω. Thus a set of related charge transfer processes, for which the effective I are about the same, have $\sigma(v)$ functions which all go to the same limit at high v [namely the resonant $\sigma(v)$ for that I]. At finite v, the difference between reactions lies primarily in $\omega=\Delta E/\hbar$. In Fig. 6(a) we have plotted the $\sigma(v)$ functions for a set of reactions with $\gamma \approx \gamma_{He}$, each curve corresponding to a different ΔE. Figures 6(b) and 6(c) show similar plots for $\gamma \approx \gamma_H$ and $\gamma \approx \gamma_{Cs}$, respectively. We wish to stress again that the calculations become less reliable at low velocities where σ is very small.

Before proceeding to compare these calculations with experiment, we must use caution because of two complications. One is that the experimental data varies over wide limits, as the scatter in measured resonant cross sections [Figs. 3(a)–(g)] indicate. The other is that the contribution of excited states, both in the primary ion beam and in the reaction products, can make obscure the exact reaction being measured. In some cases involving large nonresonances ΔE, it is possible that some reactions involving excited states have smaller ΔE, and are therefore more important than the ground state reaction considered in the two-state approximation. A set of reactions which eliminates excited ions in the primary ion beam is the reactions of protons with rare-gas atoms. Unfortunately the rare-gas ions[32] may be formed in either $^2P_{\frac{1}{2}}$ or $^2P_{\frac{3}{2}}$ states, and the energy splitting between these states is appreciable for the heavier atoms. Since two products can be formed with different values of ΔE, even in the two-state approximation, there is a duality in the calculations. It seems likely from first principles that both

[31] Although there is some ambiguity in the choice of I in a nonresonant process, σ is not usually very dependent on this choice. For extreme nonresonances such as

$$Cs+He^+ \rightarrow He+Cs^+,$$

the choice of I is both important and dubious, and the present method is inadequate.

[32] Excepting He^+, which is a ^2S state.

reactions may be possible, and that the one with the smaller ΔE are most important. For the lighter rare gases, little ambiguity exists. It is only for Kr and Xe that serious problems are encountered.

Figure 7 shows the available experimental $\sigma(v)$ for the processes

$$H^+ + He(^1S) \rightarrow He^+(^2S) + H(^2S) + H(^2S) - 11.0 \text{ eV} \quad (56)$$

$$H^+ + Ne(^1S) \rightarrow Ne^+(P_{\frac{3}{2}}) + H(^2S) - 7.9 \text{ eV} \quad (57a)$$

$$\searrow \quad Ne^+(P_{\frac{1}{2}}) + H(^2S) - 8.0 \text{ eV} \quad (57b)$$

$$H^+ + Ar(^1S) \rightarrow Ar^+(P_{\frac{3}{2}}) + H(^2S) - 2.1 \text{ eV} \quad (58a)$$

$$\searrow \quad Ar^+(P_{\frac{1}{2}}) + H(^2S) - 2.3 \text{ eV}. \quad (58b)$$

The f factors for these reactions are all unity in the forward direction. On the same plot are shown the calculated nonresonant curves for $\gamma \approx \gamma_H$ (Fig. 6(a) extended to higher velocities). While there is some latitude in the choice of γ, this is not a critical factor in the calculations. Considering the reliability of the data, it is seen that the theory correctly predicts the qualitative shapes of the $\sigma(v)$ curves, the rough absolute values of σ, and the approximate positions of the maxima. The available data for the analogous processes

$$H^+ + Kr(^1S) \rightarrow Kr^+(P_{\frac{3}{2}}) + H(^2S) - 0.4 \text{ eV} \quad (59a)$$

$$\searrow \quad Kr^+(P_{\frac{1}{2}}) + H(^2S) - 1.0 \text{ eV} \quad (59b)$$

$$H^+ + Xe(^1S) \rightarrow Xe^+(P_{\frac{3}{2}}) + H(^2S) + 1.5 \text{ eV} \quad (60a)$$

$$\searrow \quad Xe^+(P_{\frac{1}{2}}) + H(^2S) + 0.2 \text{ eV} \quad (60b)$$

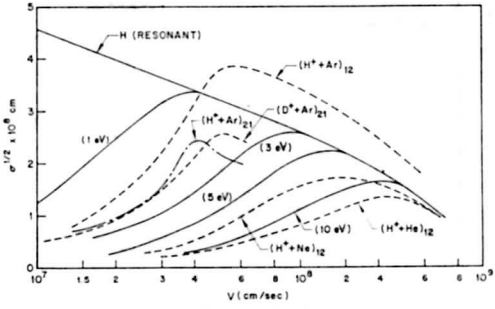

FIG. 7. Comparison of the experimental $\sigma(v)$ for reactions (56), (57), and (58), (having respective ΔE's of 11.0, 8.0, 2.2 eV) with the theoretical $\sigma(v)$ curves (extended to higher velocity) from Fig. 6(b) for various ΔE and $\gamma = \gamma_H$. The maxima occur in the correct velocity regions, the order of magnitude of σ is (very roughly) correct, and the qualitative shapes of the $\sigma(v)$ curves agree with theory quite well. The theoretical curves are solid lines and the experimental curves are broken lines, the subscripts 12 and 21 referring to experimental references in Table II.

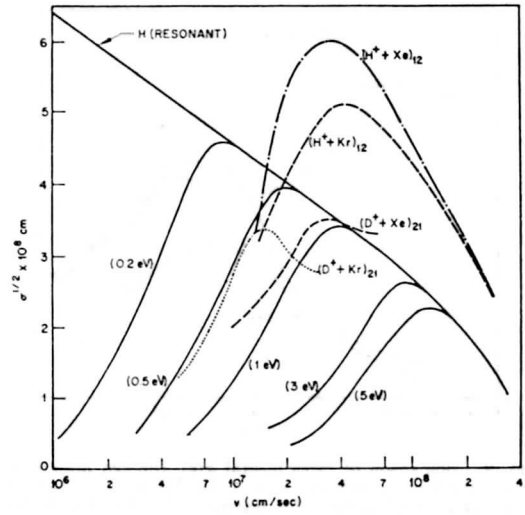

FIG. 8. Comparison of the experimental $\sigma(v)$ for reactions (59) and (60) with the theoretical $\sigma(v)$ curves taken from Fig. 6(b) with $\gamma = \gamma_H$. In the reaction with Xe there seems to be evidence only of reaction (60a), whereas two separate experiments with Kr seem to lead to reaction (59a) in one case, and reaction (59b) in the other. It is difficult to say which reactions were taking place in the experiments, so that a comparison with the theory is dubious.

are plotted in Fig. 8, along with the calculated nonresonant curves for $\gamma \approx \gamma_H$. The large difference in ΔE between reactions producing $P_{\frac{3}{2}}$ and $P_{\frac{1}{2}}$ rare-gas ions makes application of the theory somewhat dubious. One might conjecture the possibility of two maxima in the $\sigma(v)$ curve. In actual experiments, the Xe data indicate only reaction (60a), whereas in separate experiments the Kr data give evidence of both reactions (59a) and (59b). It is difficult to draw any definite conclusions because of the scatter in the data, and the exact reactions studied are difficult to ascertain.

The reactions of He^+ with the rare-gas atoms also provide a series of related processes which can be compared with our calculations. Only the processes

$$He^+ + Ne \rightarrow He + Ne^+ + 3.0 \text{ eV} \quad (61)$$

and

$$He^+ + Ar \rightarrow He + Ar^+ + 8.8 \text{ eV} \quad (62)$$

are considered. The data for Kr show evidence of excited states participating, and we have not included them here. The data for reaction (61) are shown in Fig. 9 along with the calculated curve from Fig. 6(a). Qualitatively the agreement is very good. The data for reaction (62) is shown in Fig. 10 along with the theoretical curves from Fig. 6(b). The agreement is not too good, but the theoretical curve has the correct type of qualitative behavior. There are data available for a number of other nonresonant processes which do not exhibit "normal" behavior.[33] Hasted[33] has shown that

[33] J. B. Hasted, Proc. Roy. Soc. (London) **A212**, 235 (1952).

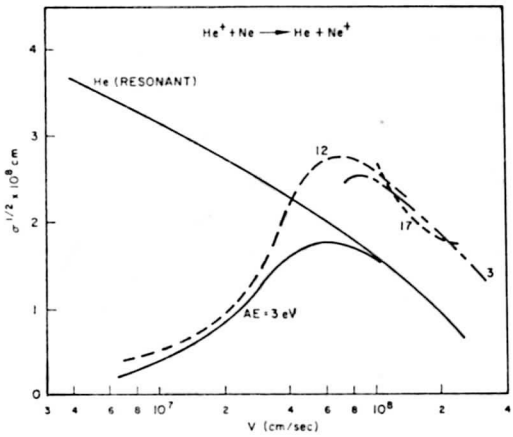

FIG. 9. Comparison of experimental $\sigma(v)$ (broken lines with numbers referring to references in Table II) with theoretical curves taken from Fig. 6(a), for reaction (61). The ΔE of this process is 3 eV. There is some error in the absolute σ, but the qualitative shape of the $\sigma(v)$ curve is correctly predicted.

in some cases one may regard the experimental data as a composite of several processes involving excited states of products and reactant ions.

One excellent test of the consistency of theory and experiment lies in a measurement of the cross sections of reverse reactions. For example, f_1/f_2 (the ratio of forward to reverse reaction cross sections at the same ion velocity) is predicted to be 4 for reaction (56) and 3 for reaction (61). There are not enough data on hand to test these predictions. There is one interesting example which shows the effect of the symmetry considerations presented in Sec. IV. This involves the relative cross sections of the processes,

$$O^+(^4S)+H(^2S)\rightarrow O(^3P)+H^+, \tag{63}$$

$$H^+ + H(^2S)\rightarrow H(^2S)+H^+. \tag{64}$$

The reaction involving O^+ has a very small ΔE, and consequently has a maximum at a very low velocity. Since O and H have nearly the same ionization potentials, the cross sections for the two processes, except for the f factor in process (63), should be roughly the same at velocities above that for the maximum σ in reaction (63). The f factor for (63) is $\frac{3}{8}$, so we predict σ_{63}/σ_{64} to be $\frac{3}{8}$ at moderate velocities. The data on these processes[34] in the region where the ion velocities overlap indicate this ratio to be about 0.35. Considering the scatter in the data, and the approximation that O and H have identical wave functions merely because they have identical ionization potentials, the agreement is excellent.

[34] W. L. Fite, R. F. Stebbings, D. G. Hummer, and R. T. Brackmann, Phys. Rev. **119**, 663 (1960); D. G. Hummer, R. F. Stebbins, W. L. Fite, and L. M. Branscomb, *ibid.* **119**, 668 (1960).

VI. LOW-VELOCITY REGION

At low velocities the orbits of the ions can no longer be assumed rectilinear with constant velocity. We do not intend in this section to deal in great detail with charge exchange at low velocities. However, for certain applications, a reasonable extrapolation procedure for extending intermediate-velocity data to low velocities is desirable. To do this rigorously, a strictly wave-mechanical treatment of the collision is called for. If the semiclassical approach is to be invoked, one should at least use the curved, varying velocity, classical orbits. Charge transfer probabilities should be calculated along these orbits, and σ calculated from Eq. (4). Rather than do this in detail, we adopt a simpler procedure. At large distances the potential between an ion and an atom is the attractive polarizability-induced dipole result $(-\alpha_B\epsilon/2R^4)$, in which α_B is the polarizability of atom B, ϵ is the electronic charge, and R is the distance between A^+ and B. One may then show[35] that the orbits as a function of b (at constant v) divide into two classes, those which produce impact, and those resulting in only grazing incidence. Although some of the grazing collisions contribute to the charge exchange, we shall neglect them and thus obtain only a lower limit for σ. The charge exchange probability in a symmetric resonant process is on the average 0.5 in impact collisions.[36] But the cross section for impact collisions is[35] $(2\pi\epsilon/v)(\alpha_B/\mu)^{\frac{1}{2}}$, in which μ is the reduced mass of the ion and atom. Thus at low velocities, the cross-section for symmetric resonant charge exchange should tend toward

$$\sigma_L=(\pi\epsilon/v)(\alpha_B/\mu)^{\frac{1}{2}}. \tag{65}$$

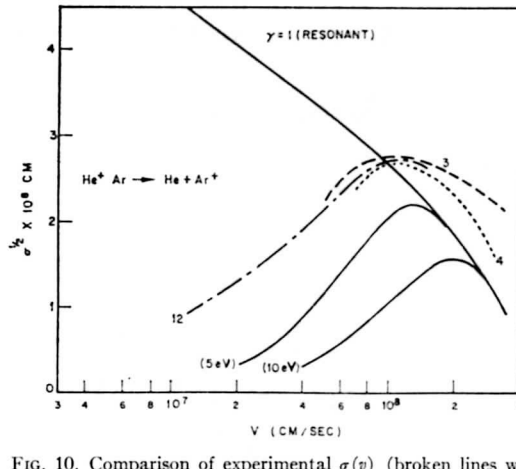

FIG. 10. Comparison of experimental $\sigma(v)$ (broken lines with numbers referring to references in Table II) with theoretical curves taken from Fig. 6(b), for reaction (62). The ΔE of this process is 8.8 eV. The theory is roughly in agreement with experiment, the major error being in the position of the maximum.

[35] D. P. Stevenson and G. Gioumousis, J. Chem. Phys. **29**, 294 (1958).

[36] The charge exchange probability may be roughly taken as $P(o, v)$ in a direct encounter, despite the curved orbit.

Since α_B tends to be of the order of 10^{-24} cm^3, this has the rough value

$$\sigma_L \cong 1.2\times 10^{-9}/(\mu^{\frac{1}{2}}v) \text{ cm}^2 \qquad (66)$$

with μ in amu, and v in cm/sec. Thus at $(\mu^{\frac{1}{2}}v)\approx 10^6$, $\sigma_L \approx 10^{-15}$ cm^2, which makes σ_L somewhat smaller than the calculated σ's presented in Fig. 2. At lower velocities, σ_L increases more rapidly than the σ's in Fig. 2, until it becomes greater. This occurs at about $(\mu^{\frac{1}{2}}v)\approx 10^5$. At lower velocities, Eq. (65) should be used. For $10^5 < (\mu^{\frac{1}{2}}v) < 10^6$, a transition zone from intermediate to low velocities exists.

In asymmetric nonresonant processes at low velocities, the main unknown is the probability of charge transfer for impact collisions, $P(o, v)$. According to Eq. (51), this would be $f/2$ instead of $1/2$ in the symmetric resonant case. However, the validity of Eq. (51) breaks down severely as $b\rightarrow 0$. It appears that $P(o, v)\ll \frac{1}{2}f$ in strongly nonresonant processes since experimental data carried down to $(\mu^{\frac{1}{2}}v)\approx 2$ to 5×10^6 show no indication of a rise in σ with decreasing v. On the other hand, there is evidence[37] from charge-exchange processes like

$$Xe^+ + C_2H_4 \rightarrow Xe + C_2H_4^+, \qquad (67)$$

in which excited electronic-vibrational levels may easily match to produce an effective near resonance, that $\sigma(v)$ roughly obeys Eq. (66) in the low-velocity region. The behavior of nonresonant $\sigma(v)$ curves at low velocities in atomic collisions remains unsettled. From the evidence in regard to reaction (67), it does appear that the near-resonant process (63) probably roughly obeys Eq. (66) (with $f=\frac{3}{8}$) below about 10^5 cm/sec. In the ionosphere, the most probable velocity for O^+-H collisions is about 5×10^5 cm/sec, which falls in the "intermediate" velocity region.

[37] J. L. Franklin and F. H. Field, Proc. ASTM Mass Spectrometry Conference, Chicago, Illinois, June 1961.

VII. CONCLUSIONS

(1) There are three ranges of ion velocity in which different treatments of charge exchange are appropriate. The "dividing lines" are at approximately $v\approx(10^5/\mu^{\frac{1}{2}})$ cm/sec and $v\approx 10^8$ cm/sec. In the "intermediate" velocity region the semiclassical impact parameter method is applicable. Most of the present work has been confined to this velocity range.

(2) A calculation of symmetric resonant charge-exchange cross sections in the intermediate velocity range has been made for a variety of atoms, in terms of their ionization potentials. This can be applied to other atoms by interpolating in terms of their ionization potentials. The agreement of the calculations with available experimental data is quite satisfactory. The method is nearly equivalent to that of reference 13, but numerical errors in that work have been corrected here.

(3) A much more approximate calculation of asymmetric nonresonant cross sections in the intermediate velocity range has been made in terms of the ΔE of the reaction and the "average" ionization potential of the two atoms. The qualitative results lead to the "near adiabatic criterion" developed previously by Massey.[18] Quantitatively, the results give the correct general variation of $\sigma(v)$, but with some error in absolute magnitude. In many cases experimental data representing processes involving excited states make it difficult to compare with our (ground state) calculations.

(4) A very brief comment on the predicted $\sigma(v)$ in the low-velocity region is presented. There are few or no experimental data for comparison.

ACKNOWLEDGMENT

One of the authors (D. R.) would like to express his appreciation to Professor J. L. Magee for many helpful discussions prior to the preparation of this manuscript.